



method. Results shows that the system can measure velocity up to 2 times higher than the conventional velocity regarding short PRT. Spatial velocity profiles estimated are obtained with a finer temporal resolution. Results are also tested under two different reception gain settings. The main purpose of this research is to develop a technique that: is computational comparable to the conventional PSE; can achieve temporal and spatial velocity resolution that is similar to the PSE; and can measure the same range of velocities of PSE but using a much longer PRT. A measurement system with similar performance of the conventional but using a longer PRT will imply in much less data to process resulting in a simpler acquisition hardware thus reducing the overall system cost. Another benefit is to achieve longer measurements range.

### 2.1.1. ST Method

#### 2.1.1.1. ST Method

In ST, an ultrasonic pulsed wave is emitted in alternating time intervals,  $T_1$  and  $T_2$ , with  $T_2 > T_1$ . Velocity estimation is evaluated by the lag one autocorrelation algorithm [7] using only adjacent pulses whose time interval is equal. The velocity relative to  $T_1$ ,  $v_1$ , and the velocity relative to  $T_2$ ,  $v_2$ , can be estimated using the following relations

$$v_1 = \frac{c}{4\pi f T_1} \arg(R(T_1)), \quad (1)$$

$$v_2 = \frac{c}{4\pi f T_2} \arg(R(T_2)), \quad (2)$$

respectively, where  $c$  denotes the sound velocity in the considered medium,  $f$  represents the transducer central frequency,  $\arg$  is the principal argument restricted to the range  $(-\pi, \pi]$  and  $R(\cdot)$  is the autocorrelation function. The maximum measured velocity is determined by the range of the principal argument as

$$v_{a1} = \frac{c}{4fT_1}, \quad (3)$$

$$v_{a2} = \frac{c}{4fT_2}. \quad (4)$$

Conventional ST method combines each lag one autocorrelation to result in a dealiased velocity estimated by

$$v_{st} = \frac{c}{4\pi f (T_2 - T_1)} (\arg(R(T_1)) - \arg(R(T_2))). \quad (5)$$

And the staggered trigger maximum velocity will be

$$v_{max,st} = \frac{c}{4f(T_2 - T_1)}, \quad (6)$$

which will be higher than Eqs. (3) and (4) if  $T_2 - T_1$  were small relatively to  $T_1$  or  $T_2$ . However, velocity estimated using Eq. (5) will have a high uncertainty for some velocity intervals [15]. Therefore, to measure velocity above Nyquist limit, Eqs. (1) and (2) should be combined to discover the velocity aliasing factor.

### 2.1.2. Velocity Aliasing Factor

The  $v_1 - v_2$  velocity difference can be used to determine the aliasing factor of  $v_1$  or  $v_2$  if the ratio  $T_1/T_2 = m/n$ , follow the condition that  $m$  and  $n$  should be relatively prime integers [14]. Applying this ratio, the maximum unambiguous velocity that can be measure are  $v_{ua1} = mv_{a1}$  and  $v_{ua2} = nv_{a2}$ , for  $v_1$  and  $v_2$ , respectively. The velocity difference rule can be demonstrated graphically. The velocity aliasing incurs that  $v_1$  or  $v_2$  cannot be higher than  $\pm v_{a1}$  or  $\pm v_{a2}$ , respectively. By plotting the real velocity versus  $v_1 - v_2$  the graph of Fig. 1 is obtained, for  $m/n = 3/4$ . Note in Fig.1, that, when  $v_1$  is aliased, or  $v_{a1} < v_1 < 3v_{a1}$ , the velocity difference assumes two unique constant values  $(-0.5v_{a1}$  and  $+v_{a1})$ . A similar behavior happens to negative aliasing in  $v_1$ , or the condition that  $-3v_{a1} < v_1 < -v_{a1}$ , in this case  $v_1 - v_2$  assumes  $+0.5v_{a1}$  and  $-v_{a1}$ . In the case of aliasing in  $v_2$ , one can notice (Fig.1) that for the first aliasing, i.e. when  $v_{a2} < v_2 < 3v_{a2}$  (or  $-3v_{a2} < v_2 < -v_{a2}$  for negative aliasing) the velocity difference assumes  $2v_{a2}$  and  $-0.5v_{a1}$  (or  $-2v_{a2}$  and  $+0.5v_{a1}$  for negative aliasing). When  $v_2$  aliases for the second time, i.e. when  $v_2 > 3v_{a2}$  (or  $v_2 < -3v_{a2}$  for negative aliasing) then  $v_1 - v_2$  equals to  $v_{a1}$  (or  $-v_{a1}$  for negative aliasing). Therefore,  $v_1 - v_2$  maps the aliasing factor in  $v_1$  or  $v_2$ . In [14] it is shown that this function bijection occurs for any  $m/n$ , if  $m$  and  $n$  are relatively prime integers.

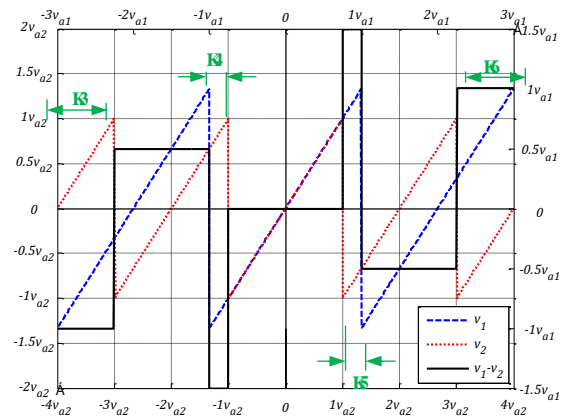


Figure 1: Velocity difference ( $v_1 - v_2$ ) and aliased velocities  $v_1$  and  $v_2$  as a function of the real Doppler velocity. Time interval ratio used was  $T_1/T_2 = m/n = 3/4$ .

### 2.1.3. Experimental Setup

To evaluate the technique, a rotating cylinder flow experiment was set-up. A plexiglass cylinder was submerged in a water tank (Fig.2). The inner cylinder radius is 70 mm. Ultrasound transducer was positioned at  $\Delta r = 20$  mm from central axis (Fig.3). With this arrangement, Doppler velocity measured by the transducer will have a uniform velocity profile (Fig.3) [1].

Rotation is established through a motor/encoder from Maxon® EPOS2 24/5. Angular speed of the motor can be configured by a software, EPOS2® Studio (Maxon®), from a computer (PC). Ultrasound control and data acquisition is performed by a PXI system from National Instruments®,

model NI5752R. The PXI system is programmed using Labview® software running in a PC. An Olympus® pulser/receiver, model 5077PR, is used for excitation and reception of ultrasound pulses from a 4 MHz transducer (Met-flow).

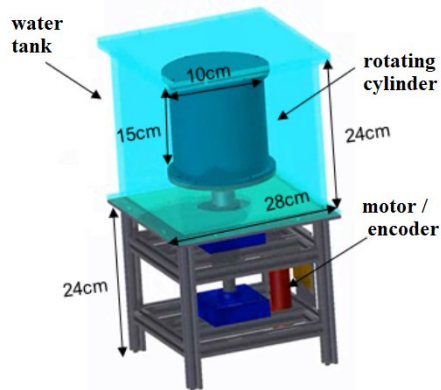


Figure 2: Rotating cylinder flow apparatus [16].

The pulser/receiver frequency was set to 1000 Hz (pulse repetition frequency). Pulse voltage used was 100 V. This pulser is limited to a 1-cycle pulse duration. Analog gain of 49 dB and 39 dB were used to amplify the echoes.

Sampling frequency of 50 MHz was set at the PXI system. A total of 2000 pulses or 2 seconds of data were recorded for each cylinder velocity tested. Cylinder rotations of 10 to 50 RPM in steps of 5 RPM were tested. A 0.5 g of nylon particles of 80 μm to 200 μm (EMS GRILTECH 1A P82), with 1.07 g/cm<sup>3</sup> were added into the cylinder. Cylinder was filled with a density matching solution of water and glycerol. Sound velocity of the solution was characterized by having the value of 1680 m/s.

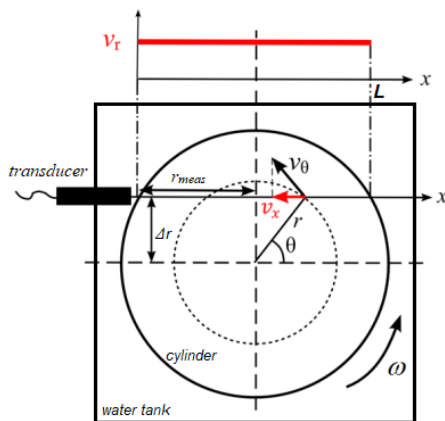


Figure 3: Top view of cylinder, transducer position and expected velocity profile. Adapted from [9].

### Methodology

Each pulse was acquired with a fixed base frequency of 1 kHz resulting in a  $T_{Base} = 1 \text{ ms}$ . To achieve a PRT ratio of  $T_1/T_2 = 2/3$ , it was adopted the following method:  $T_1 = 2T_{Base}$  and  $T_2 = 3T_{Base}$ . So, with all the 2000 RF pulses sampled (or 2 seconds of data), to transform this uniform sampled data to a non-uniform set, the system takes the first pulse, ignores the second pulse, takes the third pulse, ignores the fourth and fifth pulse and takes the

sixth pulse repeating this procedure for all pulses.

Clutter filtering of a ST data cannot be done by a standard algorithm for uniform sampled data. Therefore, stationary echoes from cylinder boundaries were filtered using a polynomial regression filter technique described in [16]. The length of the polynomial regression filter used was  $M_f = 30$ . A second order polynomial was chosen.

Velocities data regarding each PRT ( $v_1$  and  $v_2$ ) were calculated every 50 emissions ( $N_{pulse} = 50$ ). Dealiasing rules were applied to velocities estimated resulting in the dealiased velocities ( $v_{1d}$  and  $v_{2d}$ ). By averaging each dealiased velocity the final flow dealiased velocity was obtained. The spatiotemporal velocity maps were post-processed using a median filter with 2x2 matrix size.

### Accuracy Assessment

To evaluate the performance of the ST, the mean value of the spatial velocity profile was calculated for PRT ratio  $T_1/T_2 = 2/3$ . In this case the maximum velocities are  $v_{a1} = 52.5 \text{ mm/s}$  or 25.06 RPM and  $v_{a2} = 35 \text{ mm/s}$  or 16.71 RPM. The mean value was computed for cylinder velocities from 10 RPM up to 50 RPM or from  $0.3989v_{a1}$  up to  $1.995v_{a1}$  (maximum velocity for 2/3 ratio is  $2v_{a1}$  or  $3v_{a2}$ ). Analog gain of the pulser was set to 49 dB and 39 dB. The technique provides a mean velocity value with error below  $\pm 5\%$  for almost the entire range (Fig.5). Cylinder velocity of  $1.995v_{a1}$  was the only value that the technique fails to measure. This behavior may be occurred because it is a velocity that is too close of the technique limit. Fig.5 also shows that the technique performance was similar considering the SNR reduction of 10 dB (39 dB).

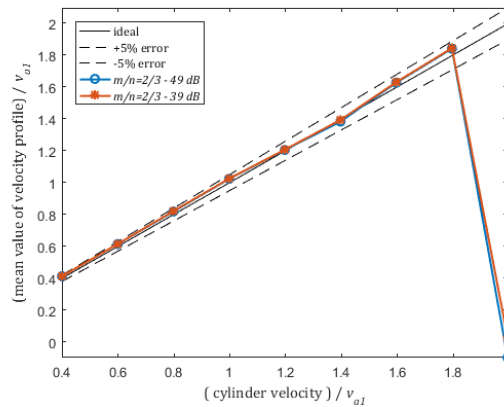


Figure 5: Accuracy assessment of ST for 2/3 ratio.

Accuracy performance of the ST was also assessed for the PRT ratio of  $T_1/T_2 = 3/4$ . In this condition the maximum velocities are  $v_{a1} = 35 \text{ mm/s}$  or 16.71 RPM. The mean value was computed for cylinder velocities from 10 RPM up to 50 RPM or from  $0.598v_{a1}$  up to  $2.992v_{a1}$  (maximum velocity for 3/4 ratio is  $3v_{a1}$  or  $4v_{a2}$ ). Analog gain of the pulser was set to 49 dB and 39 dB. Results of Fig.6 indicate that, in this case, the technique fails before the theoretical maximum. At cylinder velocity of  $2.693v_{a1}$  the error is far beyond the 5% error line. The condition is the same for 49 dB or 39 dB, possible showing that the

limitation is not on SNR.

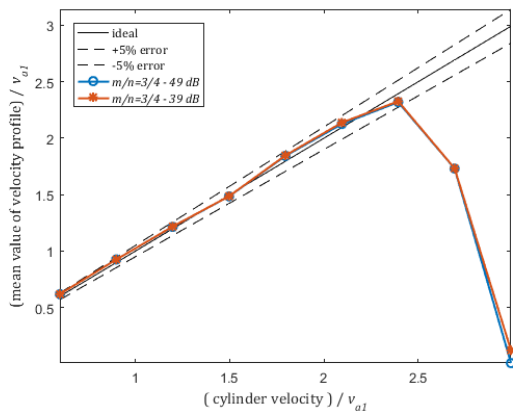


Figure 6: Accuracy assessment of ST for 3/4 ratio.

Spatial profile reproducibility is assessed in Fig. 7. It can be noticed that when velocity approaches 2 times Nyquist standard deviation (error bars) increases. Also, the polynomial regression filter fails to filter some stationary echoes from cylinder walls ( $x/L \approx 0.05$  and  $x/L \approx 0.95$ ).

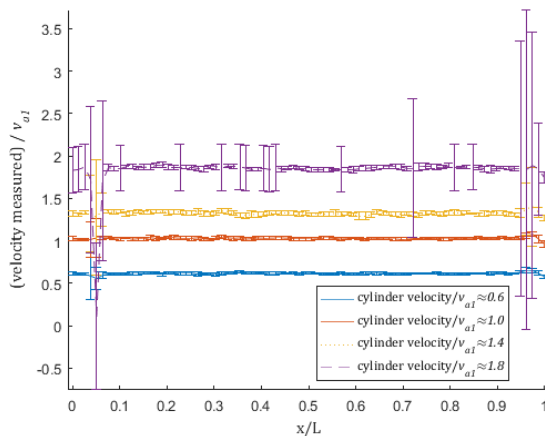


Figure 7: Spatial velocity profiles with errorbar (49 dB, 2/3 ratio).

A velocity temporal series for  $x=0.08L$  was obtained to evaluate the time accuracy of the technique. The average error relative (AER) to cylinder velocity (CV) and standard deviation normalized by  $v_{ai}$  (STD) is shown in Tab. 1.

Table 1: Temporal series accuracy results (49 dB,  $N_{pulse}=50$ ).

CV/ $v_{ai}$	0.6	0.8	1.0	1.2	1.4	1.6	1.8
AER (%)	2.4	2.6	3.0	-0.9	-3.7	1.9	3.2
STD	0.08	0.09	0.06	0.03	0.06	0.14	0.06

## Discussion

A Doppler measurement system and signal processing algorithms for ST were developed and tested in a real flow situation. Results shows that the system can measure velocities beyond Nyquist limit with accuracy of less than 5% for  $T_1/T_2 = 2/3$ . Also, the system can measure velocity with a reduced value of pulses ( $N_{pulse} = 50$ ) or

with a finer temporal resolution, thus enabling the system to be used for fast transient flow analysis. Increasing the ST ratio to  $T_1/T_2 = 3/4$  showed that the accuracy of the mean velocity value degrades as it surpasses two times the maximum conventional velocity. Therefore, for the experimental conditions tested, the ratio of 2/3 would be the best choice for application of the technique proposed because it will result in accurate velocity profiles. In the previous work of [15] higher PRT ratios were feasible to use with good accuracy. We think that it might be related to the size of the measurement volume. In [15], the ultrasound was excited by a 4-cycle pulse that is four times larger than the excitation used in this work. In a future work, we intend to test the system in pipe flows. Also, we intend to investigate if exists a tradeoff between the number of cycles emitted and the PRT ratio concerning the accuracy of velocity profiles.

## References

- [1] Takeda Y: Ultrasonic Doppler fluid flow, Springer, (2012).
- [2] Fer R, *et al.*: New Advances in colour flow mapping: quantitative velocity measurement beyond Nyquist limit. Br J Radio 64 (1991), 651.
- [3] Nitzpon HJ, *et al.*: A new pulsed wave Doppler ultrasound system to measure blod velocities beyond Niquist limit. IEEE Trans Ultrason. Ferroelec. Freq. Contr. 42 (1995), 265-279.
- [4] Zedel L & Hay AE: Design and performance of a new Multi-frequency coherent Doppler profiler. 33rd IAHR Congress, 2009.
- [5] Torp H & Kristoffersen K: Velocity matched spectrum analysis: a new method for suppressing velocity ambiguity in pulsed-wave Doppler. Ultrasound Med. Biol. 21(1995), 937-944.
- [6] Jensen, JA: Estimation of blood velocities using ultrasound: A signal processing approach. Cambridge Univ. Press, (2006).
- [7] Lai X & Torp H: An Extended Autocorrelation Method for Estimation of Blood Velocity, IEEE Trans. Ultrason., Ferroelec., Freq. Contr. 44 (2007), 1332-1342.
- [8] Ofuchi, CY, *et al.*: Extended autocorrelation velocity estimator applied to fluid engineering, Proc. of the 9th ISUD, Strasbourg (2014), 109-112.
- [9] Ofuchi C. Y. et al. Evaluation of an extended autocorrelation phase estimator for ultrasonic velocity profiles using nondestructive testing systems. Sensors. 16 (2016), 1250.
- [10] Nishiyama H & Katakura K. Non-equally-spaced pulse transmission for non-aliasing ultrasonic pulsed Doppler measurement, J. Acoust. Soc. Jpn. 13, 4 (1992), 215-222.
- [11] Franca MJ & Lemmin U: Eliminating velocity aliasing in acoustic Doppler velocity profiler data, Meas. Sci. Tech. 17 (2006), 313-322.
- [12] Holleman I & Beekhuis H: Analysis and Correction of Dual PRF Velocity Data, J. Atmos. Ocean. Tech. 20 (2003), 443-453.
- [13] Murakawa H, *et al.*: Higher flowrate measurement using ultrasonic pulsed Doppler method with staggered trigger. Proc. of ISUD9, Strasbourg (2014), 117-120.
- [14] Torres SM & Dubel Y: Design, implementation, and demonstration of a staggered PRT algorithm for the WSR-88D. J. Atmos. Oceanic Tech. 21 (2004), 1389-1399.
- [15] Coutinho, F. R. Implementation of a staggered trigger algorithm by velocity difference dealiasing rules. Proc. of ISUD10, Tokyo (2016), 45-48.
- [16] Bostelmann P. Ultrasonic instrumentation for characterization of the process of hydrate formation. Msc Thesis. CPGEI – Federal University of Technology -Parana (2016).
- [17] Torres S. M. & Zrníc D. S.. Ground clutter cancelling with a regression filter. J. Atmos. Ocean. Tech. 16 (1999), 1364-1372.